

# AEROELASTIC INVESTIGATION OF HINGELESS HELICOPTER ROTOR IN HOVER

Michael TODOROV<sup>1</sup>

Ivan DOBREV<sup>2</sup>

Fawaz MASSOUH<sup>2</sup>

Cvetelina VELKOVA<sup>1</sup>

michael.todorov@tu-sofia.bg ivan.dobrev@hotmail.com fawaz.massouh@ensam.eu tsveti@TF10109-1.tu-sofia.bg

Department of Aeronautics, Technical University of Sofia, Sofia -1000, BULGARIA  
Laboratory of Fluids Mechanics, Arts et Metiers ParisTech, Paris-7513, FRANCE

*An aeroelastic modelling of pattern hingeless helicopter rotor in hover is presented in this paper. The coupled aeroelastic problem accounts for the mutual dependence between blade structure and rotor aerodynamics. The aerodynamic model uses Blade Element Momentum Theory (BEMT). BEMT gives good accuracy with respect to time cost. The structure model uses Finite Element Method (FEM). The investigation is based on the well-known solvers MATLAB and ANSYS. The obtained results show that the proposed modeling is efficient, rapid and gives reliable results. This modelling is also useful and applicable for airplane propellers, wind turbine rotors and airplane wings.*

**Key Words:** helicopter, aeroelasticity, aerodynamics, structural dynamics

## 1. Introduction

Aerodynamic and inertia forces act on the helicopter blade in flight. These forces deform the helicopter blade and as a result, the aerodynamic forces distribution changes. The new aerodynamic forces distribution deforms the blade. In addition, that changes the aerodynamic forces distribution again. At a certain instant the aerodynamic and inertia forces, and elasticity forces will be balanced. Therefore the fully coupled aeroelastic problem must account for the mutual dependence between blade structure and aerodynamics.

The last years of researches have provided significant successes in the prediction of airloads on the helicopter rotors. These predictions are based on a numerical approach, where the flow is simulated using Computational Fluid Dynamics (CFD) tools with moving boundary conditions. The computations normally include a comprehensive rotor code, coupled to Euler or Navier-Stokes solvers [Datta 2004, Servera 2002, Righi 2010]. The examples for a successful application of CFD are the codes FLUENT, TURNS of NASA, FLOWer of Deutsches Zentrum für Luft und Raumfahrt, elsA and WAVES of ONERA [Servera 2002]. For aeroelastic calculations the CFD method has to be very time consuming. Thus it can be replaced by Blade Element Momentum Theory (BEMT) or the vortex wake method which show a good accuracy with respect to time cost [Leishman 2000]. In these methods, the helicopter blade is divided into a number of independent elements

along the length of the blade. Each section of the blade acts as quasi 2-D airfoil, which produces aerodynamic forces and moments.

The structure of helicopter blade has been modelled in different ways but mostly relies on a modified beam model or one-dimensional finite elements [Righi 2010].

The lumped-parameter approach is used to determine the helicopter blade deformations under the effects of aerodynamic and inertia forces. There the continuous blade is presented by a number of discrete segments, so that the partial differential equations of blade deformations are replaced by a set of simultaneous ordinary differential equations. The methods using this approach are the Holzer-Myklestad method [Bramwell 2001], collocation method [Bielawa 1992] and Finite Element Method (FEM) [Bielawa 1992, Floros 2000, Shen 2003]. The FEM solvers as ANSYS, ABAQUS, NASTRAN and ADAMS are often applied at the investigations of helicopter rotor dynamics.

The advanced helicopter code called UMARC is well validated and extensively used in the helicopter rotor dynamics investigations. The rotor-fuselage equations are formulated using Hamilton's principle and are discretized using finite elements in space and time. The blade airloads can be computed using quasi-steady aerodynamics, linear unsteady aerodynamics or nonlinear unsteady aerodynamics [Bir 1990, Freidmann].

Other successful helicopter code is CAMRAD. The used model is a combination of structural,

inertial, and aerodynamic models. The rotor aerodynamic model is based on free vortex method, which takes in account the unsteady flow effects, including a dynamic stall [Johnson 1988, Freidmann 2004].

The aim of this work is to present an aeroelastic investigation of hingeless helicopter rotor. The structural model uses FEM, and aerodynamic model uses BEMT. The structural model relies on ANSYS code, and aerodynamic model relies on MATLAB code.

### 2. Structural model of a hingeless helicopter rotor

The advantage of hingeless rotor is its mechanical simplicity. It eliminates the flapping and lead/lag hinges by using an elastic element or elastic blade to accommodate blade motion. But the design

of the blade in most cases is rather complicated. The sketch of a hingeless rotor is shown in Fig.1.

An ANSYS code is used for the structural analysis. The equivalent beam model of the helicopter blade uses finite element BEAM44 (Table 1). The element has six degrees of freedom at each node: translations in the nodal  $x$ ,  $y$ , and  $z$  directions and rotations about the nodal  $x$ ,  $y$ , and  $z$ -axes. This element uses different asymmetrical geometry without coinciding centre of gravity and elastic centre. The blade is divided into 21 finite elements, as shown in Table 1. The material of the blade hub is Aluminum 7079, the elastic element is from stainless steel AISI 304, and the blade is from balsa. All necessary data are shown in Table 1. The transient analysis solution method is used and gyroscopic or Coriolis effects are included.

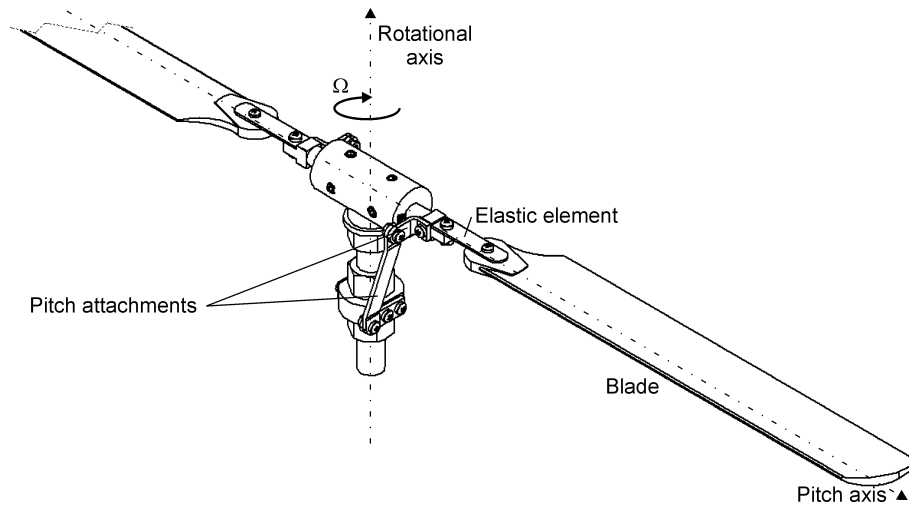


Fig. 1 Sketch of a pattern hingeless rotor

### 3. Loads on the helicopter blade

In hovering flight, the flow field is steady in coordinate system which rotates with the rotor and has rotational periodicity. This is the easiest flow regime for mathematical modeling and analysis. The blade element momentum theory (BEMT) gives the basis of most analyses of rotor aerodynamics. When it's used a part of aeroelastic codes, this method is very time efficient and gives good accuracy with respect to time cost.

In this method, the helicopter blade is divided into a number of independent elements along the length of the blade. At each blade element, a force balance is applied involving 2D blade section lift and drag with the thrust and torque produced by the element. At the same time, a balance of axial and angular momentum is applied. The force balances produce a set of non-linear equations which can be solved numerically for each blade section. The description follows [Leishman 2000].

Fig. 2 shows the incident velocities and aerodynamic forces at a blade element on the helicopter rotor.

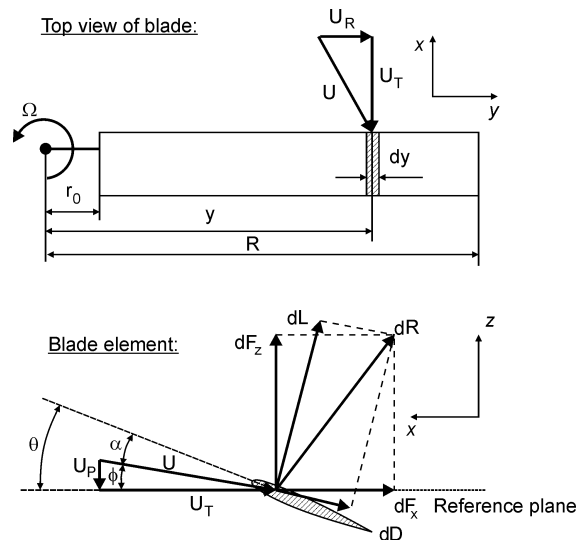


Fig. 2 Incident velocities and aerodynamic forces at a blade element

Table 1 Description of the structural helicopter rotor FEM model

<p><u>Rotor sketch</u>, shown dimensions are in (mm)</p>					
<p><u>Section properties:</u> Section area, <math>A</math>, m Inertia moment about the <math>x</math> axis, <math>I_{xx}</math>, m<sup>4</sup> Inertia product, <math>I_{xz}</math>, m<sup>4</sup> Inertia moment about the <math>y</math> axis, <math>I_{yy}</math>, m<sup>4</sup> <math>x</math> coordinate of shear center about c.g., <math>x_{sc}</math>, m <math>z</math> coordinate of shear center about c.g., <math>z_{sc}</math>, m</p>	<p><b>A</b></p> <p><math>0.452 \times 10^{-3}</math> <math>0.163 \times 10^{-7}</math> 0.000 <math>0.163 \times 10^{-7}</math> 0.000 0.000</p>	<p><b>B</b></p> <p><math>0.636 \times 10^{-4}</math> <math>0.321 \times 10^{-9}</math> 0.000 <math>0.321 \times 10^{-9}</math> 0.000 0.000</p>	<p><b>C</b></p> <p><math>0.810 \times 10^{-4}</math> <math>0.547 \times 10^{-9}</math> 0.000 <math>0.547 \times 10^{-9}</math> 0.000 0.000</p>	<p><b>D</b></p> <p><math>0.180 \times 10^{-5}</math> <math>0.600 \times 10^{-14}</math> 0.000 <math>0.122 \times 10^{-10}</math> 0.000 0.000</p>	<p><b>E</b></p> <p><math>0.106 \times 10^{-3}</math> <math>0.127 \times 10^{-9}</math> 0.000 <math>0.127 \times 10^{-9}</math> 0.002 0.000</p>
<p><u>Finite element model:</u> Nodes: 1-21 Elements: 1-21</p>					
<p><u>Elements Type:</u></p>	<p style="text-align: center;"><b>BEAM 44</b></p>				
<p><u>Material properties:</u>  Elastic modulus, <math>E_x</math>, GPa Elastic modulus, <math>E_y</math>, GPa Elastic modulus, <math>E_z</math>, GPa Shear modulus, <math>G_{xy}</math>, GPa Shear modulus, <math>G_{xz}</math>, GPa Shear modulus, <math>G_{yz}</math>, GPa Density, <math>\rho</math>, kg/m<sup>3</sup></p>	<p>Elements: 1-3 Aluminum 7079, isotropic material 71.7  26.9  2800</p>	<p>Element: 4 Stainless steel AISI 304, isotropic material 190  79  8000</p>	<p>Elements: 5-21 Wood: Balsa, orthotropic material 3.400 0.156 0.051 0.183 0.126 0.017 160</p>		

As is shown in Fig.2, the resultant flow velocity at each blade element at a radial distance  $y$  is

$$(1) \quad U = \sqrt{U_T^2 + U_p^2}$$

where  $U_T = \Omega y$  and  $U_p = v_i$ . The induced angle of attack (inflow angle) at the blade element is

$$(2) \quad \phi = \tan^{-1} \left( \frac{U_p}{U_T} \right)$$

The averaged induced velocity is connected with the inflow ratio

$$(3) \quad \lambda = \frac{v_i}{\Omega R} = \phi r$$

where  $r=y/R$ .

The effective angle of attack is

$$(4) \quad \alpha = \theta - \phi$$

where  $\theta$  is the pitch angle at the blade element.

When there is torsional elastic deformations of the blade,  $\theta_e$ , the effective angle of attack is

$$(5) \quad \alpha = \theta - \phi + \theta_e$$

The resultant lift  $dL$  and drag  $dD$  per unit span on the blade element are

$$(6) \quad dL = \frac{1}{2}\rho U^2 c C_l dy \quad \text{and} \quad dD = \frac{1}{2}\rho U^2 c C_d dy$$

where  $\rho$  is the density of air,  $c$  is the local blade chord,  $C_l$  and  $C_d$  are the lift and drag coefficients.

Based on steady linearized airfoil aerodynamics, the local blade lift coefficient can be written as

$$(7) \quad C_l = C_{l_\alpha} (\alpha - \alpha_0)$$

where  $C_{l_\alpha}$  is the 2-D lift-curve-slope of airfoil section, and  $\alpha_0$  is the corresponding zero-lift angle. The effects of compressibility corrects the lift-curve-slope of each blade element according to Glauert's rule

$$(8) \quad C_{l_\alpha} = \frac{C_{l_\alpha}|_{M=0.1}}{\sqrt{1-M^2}}$$

$C_{l_\alpha}|_{M=0.1}$  is the measured 2-D lift-curve-slope at  $M=0.1$ . The local blade Mach number is

$$(9) \quad M = \frac{U_T}{a} = \frac{\Omega y}{a}$$

where  $a$  is the sonic velocity.

The inflow ratio is obtained by the use of Prandtl's tip-loss method

$$(10) \quad \lambda = \frac{\sigma C_{l_\alpha}}{16F} \left( \sqrt{1 + \frac{32F\theta r}{\sigma C_{l_\alpha}}} - 1 \right)$$

where  $\sigma = \frac{N_b c}{\pi R}$  is the rotor solidity, and  $N_b$  is the number of rotor blades. The Prandtl's factor,  $F$ , corrects the induced velocity

$$(11) \quad F = \left( \frac{2}{\pi} \right) \cos^{-1}(e^{-f})$$

and

$$(12) \quad f = \frac{N_b}{2} \left( \frac{1-r}{r\phi} \right)$$

Because  $F$  is a function of  $\lambda$ , the Eq.11 must be solved iteratively. For first iteration  $F=1$  (corresponding to an infinite number of blades) and then finding  $F$  from Eq.11 and recalculating  $\lambda$  from

the numerical solution to Eq.10. Convergence is obtained in 3 or 4 iterations.

Finally the forces perpendicular and parallel to the rotor disk are

$$(13) \quad dF_z = dL \cos \phi - dD \sin \phi$$

$$(14) \quad dF_x = dL \sin \phi + dD \cos \phi$$

The equilibrium of the blade depends by the balance of aerodynamic and centrifugal forces. In accordance with Fig. 3, a small element of the blade of length  $dy$  is considered. The mass of this element is  $m dy$ . The centrifugal force acting in a parallel direction to the plane of rotation is

$$(15) \quad d(F_{CF}) = m\Omega^2 y dy$$

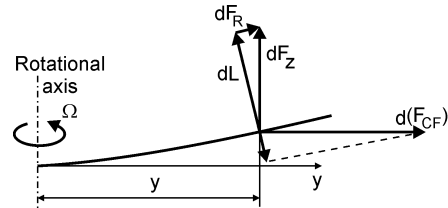


Fig. 3 Equilibrium of blade element aerodynamic and centrifugal forces

Because the aerodynamic center and shear center not coincident, reference to classical airfoil theory gives the section moment  $dM_x$ , as taken about shear center, defined in Fig.4

$$(16) \quad dM_x = \frac{1}{2}\rho U^2 c C_l x_{sc} dy$$

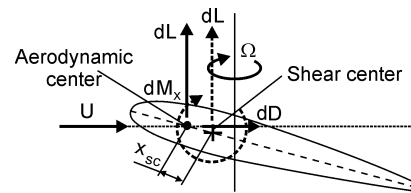


Fig.4 Section moment relevant geometry of a blade element

The helicopter airfoil is NACA 0012. The airfoil data for NACA 0012 are presented in [Sheldahl 1981]. The rotor angular velocity,  $\Omega$ , is 50 rad/s. The blade chord is 0.032 m. The blade has not linear twist. The blade pitch angle is  $5^\circ$ . The aerodynamic loads are calculated by MATLAB code.

#### 4. Numerical results

The algorithm of the coupling between the structural model and aerodynamic model is:

1. The aerodynamic forces are computed for an ideal rigid blade by MATLAB code;
2. The aerodynamic and inertia forces are applied on the blade FEM-model by code ANSYS;
3. The linear and angular blade deformations are computed by ANSYS code;
4. The new angle of attack for each element of the blade is computed and new distribution of the aerodynamic forces is received by MATLAB code for second iteration;
5. The new aerodynamic and inertia forces are applied on the FEM-model by ANSYS code;
6. The new linear and angular blade deformation are calculated by ANSYS code;
7. The new distributions of the aerodynamic forces and deformations are compared;
8. If they are changed more than a certain tolerance: go to step 4;
9. The iteration is repeated while a convergence is achieved.

The results are shown in Figs.5-8. Fig.5 shows the vertical bending deformation and Fig.6 shows the torsional deformation of the helicopter blade in the nodes. The results are obtained by ANSYS code. Fig.7 shows the lift distribution, and Fig.8 shows drag distribution, as the results are obtained by MATLAB code.

Five iterations of helicopter rotor are made while a divergence has achieved. The drag influences depends weakly from elastic properties of the blade in hover. Consequently, it is necessary to render an account of the blade elasticity at the calculations of the helicopter rotor thrust, torque and power in hover. In addition the aeroelastic effects will influence on the strength calculations of rotor sturcture.

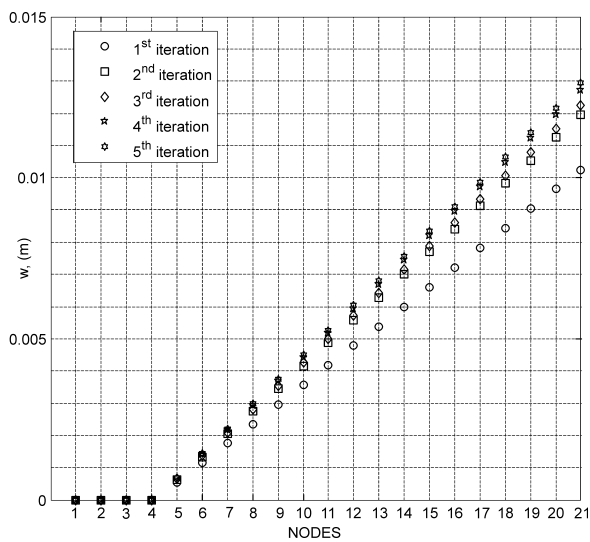


Fig. 5 The bending vertical deformation,  $w$ , in the nodes

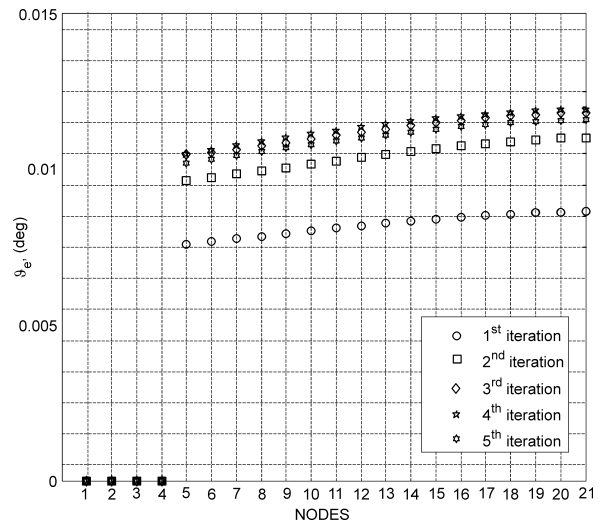


Fig.6 The torsional deformation,  $\theta_e$ , in the nodes

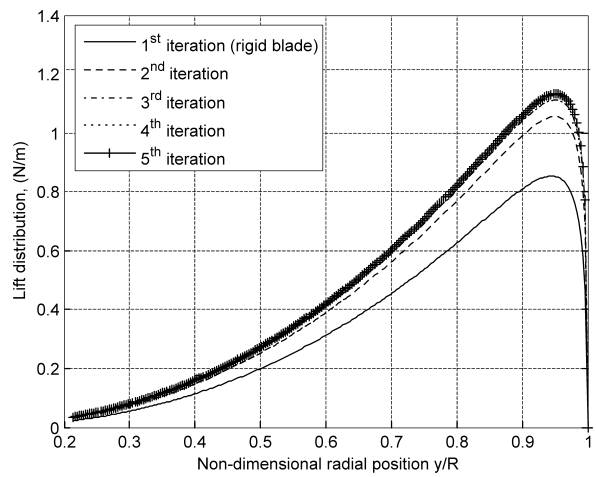


Fig.7 The lift distribution,  $dL$

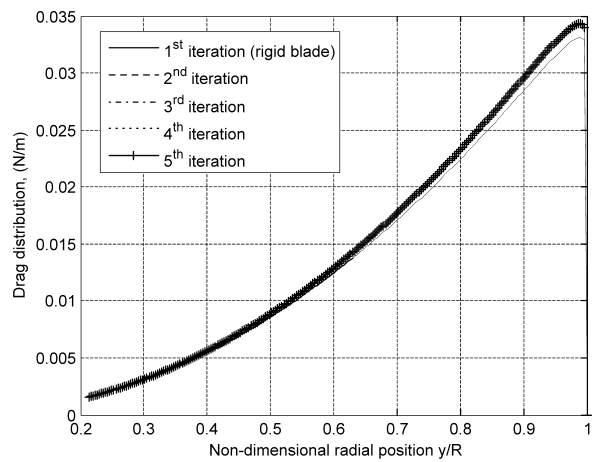


Fig.8 The drag distribution,  $dD$

Fig.9 shows the coning (flapping up) angle of the helicopter rotor at the final iteration.

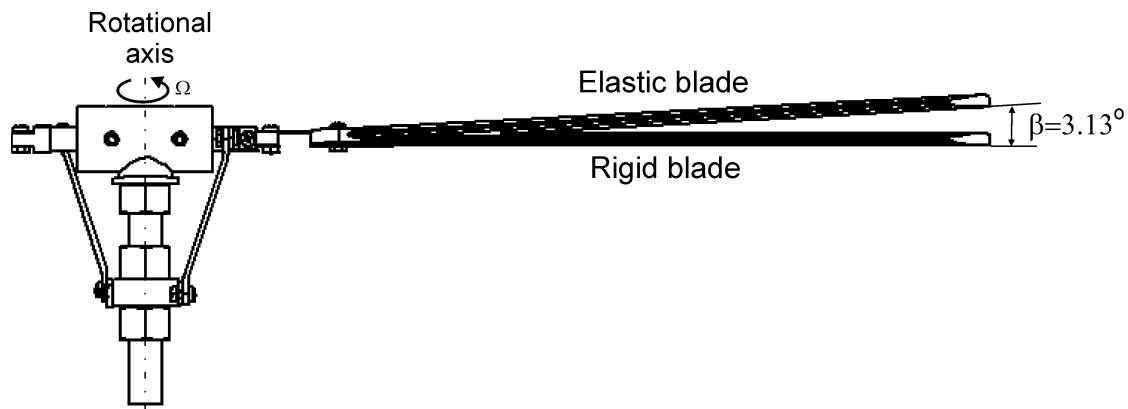


Fig. 9 Coning angle

## 5. Conclusion and future works

A simple aeroelastic modelling of pattern helicopter hingeless rotor in hover, which uses well-known solvers MATLAB and ANSYS, was presented in this paper. The effective and fast BEMT method was applied to create an aerodynamic model. To analyse the aeroelastic behaviour of helicopter rotor the FEM method is used, as the blade was presented with equivalent beam model. The results confirm that the centrifugal forces are dominant and the coning angle of the helicopter rotor remains small.

The future work provides for the aeroelastic modelling to be made in forward flight. An experiment in a wind tunnel will also be provided for.

## Acknowledgements

This study has been supported by Research and Development Direction of Technical University of Sofia (Grant 122PD0001-04/2012).

## Bibliography

Bielawa R.L., Rotary Wing Structural Dynamics and Aerolasticity, AIAA Educational Series, 1992

Bir G., Chopra I., and Nguyen K., Development of UMARC, 46<sup>th</sup> Annual National Forum of the American Helicopter Society, D.C, May, 1990

Bramwell A.R.S., Done G., and Balmford D., Bramwell's Helicopter Dynamics, Butterworth-Heinemann, 2001

Datta A., Fundamental Understanding, Prediction and Validation of Rotor Vibratory Loads in Steady-Level Flight, Dissertation, University of Maryland, 2004

Floros M., Elastically Tailored Composite Rotor Blades for Stall Alleviation and Vibration Reduction, Dissertation, Pennsylvania State University, 2000

Freidmann P.P., Rotary-Wing Aeroelasticity: Current Status and Future Trends, AIAA Journal, vol.42, No10, October 2004, pp.1953-1971

Johnson W., Recent Developments in Rotary-Wing Aerodynamic Theory, AIAA Journal, vol.24, No8, August 1986, pp.1219-1243

Johnson W., CAMRAD: A Comprehensive Analytical Model of Rotorcraft Aerodynamics and Dynamics, Johnson Aeronautics, 1988

Johnson W., Helicopter Theory, Dover Publications, New York, 1994

Johnson W., Rotorcraft Dynamics Models for a Comprehensive Analysis, American Helicopter Society 54<sup>th</sup> Annual Forum, DC, May 20-22, 1998

Leishman J.G., Principles of Helicopter Aerodynamics, Cambridge University Press, 2000

Righi M., Application of Computational Aeroelasticity to Design of Helicopter Rotor Blades, 27<sup>th</sup> International Congress of The Aeronautical Sciences-ICAS 2010

Sheldahl R.E., Aerodynamics Characteristics of Seven Airfoils Sections through 180 Degrees Angle of Attack for Use in Aerodynamic Analysis of Vertical Axis Wind Turbines, SAND80-2114, Sandia National Laboratories, Albuquerque, New Mexico, March 1981

Servera G., Developpement d'une Methodologie de Couplage Dynamique/Aerodynamique pour les Rotors d'Helicoptere, These, Universite d'Orleans, 2002

Shen J., Comprehensive Aeroelastic Analysis of Helicopter Rotor with Trailing-Edge Flap for Primary Control and Vibration Control, Dissertation, University of Maryland, 2003